Journal of Computer Science & Computational Mathematics, Volume 6, Issue 1, March 2016
DOI: 10.20967/jcscm.2016.01.001

Finite Element Analysis of Precast Lightweight Foamed Concrete Sandwich Panel Subjected to Axial Compression

W. I. Goh[1], N. Mohamad[2*], R. Abdullah[3], A. A. A. Samad[4]

[1,2,4]Universiti Tun Hussein Onn Malaysia, Batu Pahat, Johor, Malaysia,
[3]Universiti Teknologi Malaysia, Skudai, Johor Malaysia,
[*]Corresponding author email: noridah@uthm.edu.my

***Abstract*:** Quasi static finite element analysis (FEA) was conducted on precast lightweight foamed concrete sandwich panel (PLFP) using ABAQUS/Explicit module to study its structural behavior. The PLFP subjected to axial load was simulated under perfect and imperfect conditions. Results from the FEA were validated with experimental data accurately. The analysis produced ultimate load carrying capacity, damage criteria and vertical and horizontal displacement. It was found that the proposed finite element model for PLFP with perfect and imperfection conditions can predict the structural behavior of PLFP accurately. Therefore, a computational study by using FEA can be used as an economical alternative tool to replace the experimental study of structural behavior of PLFP.

***Keywords*:** Finite element analysis, sandwich panel, geometrical imperfection, quasi static analysis**.**

1. Introduction

It is a common practice in the design of column to allow certain amount of geometric imperfections due to fabrication and erection tolerances. Among previous researches, Artizabal-ochoa [1] has completed a series of analytical study for stability and second order non-linear analysis of 2D multi-column system to study the effects of initial imperfections. The research found out the effect of initial imperfections on the induced bending moments, second order deflections and buckling axial loads of plane in the structure. The results indicated that the stability and second order respond in multi-column system are highly affected by the shape, magnitude and direction of the initial imperfections, end fixities, lateral bracing, and axial load distribution among the columns. Unlike an ideal system with perfect straight and vertical column loaded concentrically (which ideally remain straight up to its critical axial load), the real system with imperfect condition begin to bend as soon as the axial loads are applied. The larger the initial imperfections and the applied axial loads, the larger the end reactions, bending moments and deflections of each column are. Boissonnade and Somja [2] investigated the influence of geometrical imperfection (both local and global) in steel girder by using FEA. More than 700 results of FEA show adequate and reasonably realistic sets of initial geometrical imperfections. They found that the initial global imperfection may affect bending the resistance of the steel girder but local imperfection did not affect the result. This is shown by the analyzing the results where the steel girder with and without local imperfection are fully coincident. In addition, the cross sections do not comprise any highly slender component, so that the influence of local buckling on the global behavior remains negligible.

This paper proceeds with providing an accurate modeling and analysis method to obtain the structural behavior of PLFP in terms of its damage criteria and ultimate load carrying capacity. Quasi static analysis available in ABAQUS/Explicit Dynamic 6.9 was implemented in order to simulate the brittle behavior of model efficiently [3]. A three dimensional non-linear finite element model of PFLP was developed and validated with experimental results. The main considerations included in the model, were concrete damage plasticity of foamed concrete and geometrical imperfection of the PLFP.

2. Structural Model

The proposed structural model of PLFP is a three dimensional (3D) nonlinear finite element model. The PLFP panels with single shear truss connector were simulated. Each parts of PLFP were modeled separately in part module in ABAQUS software by using different types of element based on the suitability of each element. The elements used for each parts are tabulated in Table 1. The modeling process including discretized geometry, element section properties, material data, load and boundary conditions, analysis types and output requests were addressed.

Table 1. Elements used for each parts of PLFP

No.	Part	Element
1	Foamed concrete	Continuum three dimensional 8 nodes linear brick element, reduced integration and hourglass control
2	Normal Concrete Capping	Continuum three dimensional 8 nodes linear brick element, reduced integration and hourglass control
3	Polystyrene	Continuum three dimensional 8 nodes linear brick element, reduced integration and hourglass control
4	Shear Connector	Three dimensional 2 nodes element

5	Main reinforcement	Three dimensional 2 nodes element

The PLFP model was initially built up with geometry discretization of each part. Due to the complex reinforcement arrangement in the panel, the steel reinforcement was simulated with three dimensional of two-node elements. The area of reinforcement was taken into the analysis with the section properties assignment of its cross section area and material properties. Additionally, section properties of each element were assigned with material data from experiments results and previously published by other researches. Rigid body was assigned at top and bottom at the panel which functioned as load transfer medium to the panel under study.

After the PLFP model was assembled, the individual modeled parts were connected properly to each other. Tie contact technique was utilized to create proper interaction between the surfaces of solid elements, with normal concrete capping, foamed concrete and polystyrene as shown in Figure 1. Tie technique (perfect bonding) was used to prevent slippage between the surfaces of the elements. The connection between the main reinforcement and shear connectors with solid elements was obtained by using embedded technique to constraint the reinforcement into solid element in order to create a proper bonding and composite action.

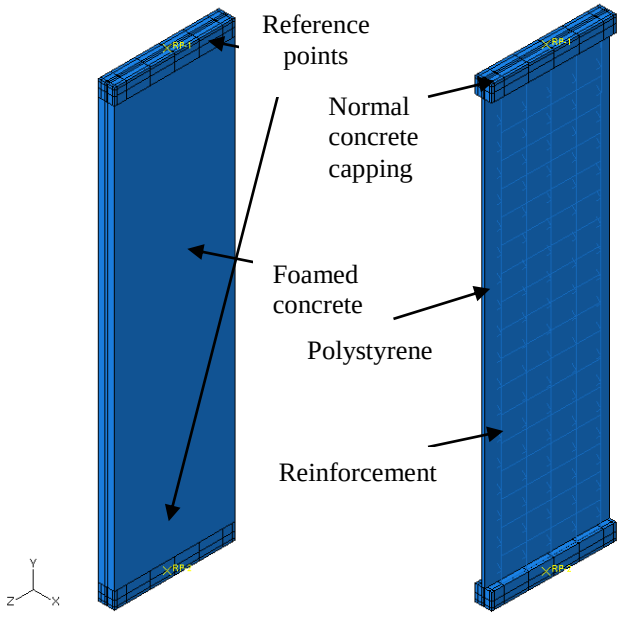

Figure 1. Structural model of PLFP

3. Material Model

The non-linear materials obtained from experiment were assigned in the element accordingly. Four types of material properties were considered, namely foamed concrete, normal concrete capping, reinforcement and polystyrene. The material properties of normal concrete and polystyrene were obtained from previous studies [4], [5], [6] & [7].

3.1 Concrete Material Model

Failure criterion for the structure is required for the analysis process. Figures 2a and 2b illustrate the concrete stress/strain relationships to correlate parameters for relative concrete damage for both tension and compression. The concrete damaged plasticity model uses concepts of isotropic damaged elasticity in combination with isotropic tensile and compressive plasticity to represent the inelastic behavior of concrete. Many previous researchers implemented concrete damaged plasticity model in their research and had proven that the model worked satisfactory [4], [8], [9] & [10].

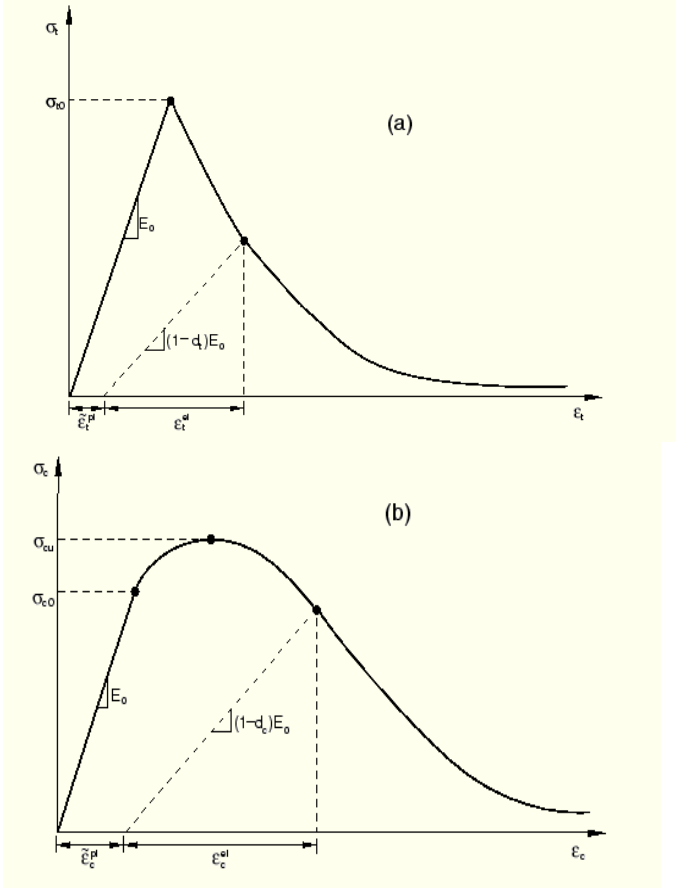

Figure 2. Response of concrete to uniaxial loading in tension (a) and compression (b) [3]

Material properties of foamed concrete were obtained from the experiment (compressive and tensile behavior) and previous researches (parameters) were used as input for concrete damaged plasticity model to the model. Series of compression test on cubes and cylinders were conducted at 28th day to get the compressive strength, Young's modulus and Poisson ratio and split tensile test on cylinders were conducted to determine the tensile strength. Compressive strength, tensile strength, Young's modulus, mass density and Poisson ratio of foamed concrete obtained from experiments have been tabulated in Table 2. Based on British Cement Association [11], all properties are comparable with typical foamed concrete material properties.

Table 2. Properties of foamed concrete in PLFP

P_c (MPa)	***F_t (Mpa)***	***E (kN/mm^2)***	***Mass Density, p (kg/m^3)***	***υ***

7.456	0.861	12	1,600	0.2

Compressive and tensile behaviors of foamed concrete were determined from experimental testing and calculated based on the stress-strain relations under uniaxial tension and compression loading in equation (1). Under uniaxial cyclic loading conditions the degradation mechanisms are quite complex, involving the opening and closing of previously formed micro-cracks, as well as their interaction. The concrete damaged plasticity model assumes that the reduction of the elastic modulus is given in terms of a scalar degradation variable *D* as

$$D = 1 - \frac{E}{E_o} \qquad (1)$$

where E_o is the initial (undamaged) modulus of the material. The stiffness degradation variable, *D*, is a function of the stress state and the uniaxial damage variables under tension and compression. Damage variables are treated as non-decreasing material point quantities. At any increment during the analysis, the new value of each damage variable is obtained as the maximum between the value at the end of the previous increment and the value corresponding to the current state [3].

Table 3 shows the constitutive parameters used in concrete damaged plasticity model for foamed concrete material. Parameters (dilatation angle, eccentricity, initial biaxial and uniaxial ratio, *K* and viscosity) listed in Table 3 that are not measurable from the experiment, were assumed using values from normal strength concrete. Due to the parameters of foamed concrete identified by previous researches; the parameters in this study were assumed based on the parameters of normal strength concrete stated by Mokhatar and Abdullah, [4] and Newberry, Hoemann, Bewick, and Davidson [5]. Compressive and tensile behavior data that are measurable from experimental testing were obtained from experimental studies and were used to calculate the damage parameter by using isotropic damage criteria in Figure 2.

Table 3. Concrete damaged plasticity of foamed concrete

Concrete Damaged Plasticity					
Dilatation Angle	Eccentricity	Initial biaxial/ uniaxial ratio, σ_{c0}/σ_{b0}		*K*	Viscosity
27°	1	1.12		1	0
Compressive Behavior			Tensile Behavior		
Yield Stress, (MPa)	Inelastic Strain	Damage Parameter, *D*	Yield Stress (MPa)	Cracking Strain	Damage Parameter, *D*
6.3	0.0000	0.000	0.861	0.00000	0.000
7.1	0.0017	0.000	0.776	0.00159	0.204
7.5	0.0033	0.000	0.605	0.00409	0.476
7.2	0.0041	0.215	0.518	0.00526	0.582
7.0	0.0047	0.337	0.431	0.00638	0.673
6.7	0.0055	0.456	0.345	0.00746	0.752
6.3	0.0066	0.577	0.259	0.00854	0.824
5.6	0.0078	0.682	0.173	0.00966	0.889
3.9	0.0127	0.862	0.086	0.01082	0.947
2.9	0.0194	0.934	0.000	0.01202	1.000

3.2 Steel Material Model

Properties used for shear connector and main reinforcement were based on the results from tensile testing in laboratory which included initial yield stress, ultimate stress; strain at failure while the Modulus' Young, mass density and Poisson ratio were assumed based on regular properties of reinforcement. The elastic and plastic steel behaviors (6mm and 9mm) were used to simulate the PLFP structural behavior. All the material properties are tabulated in Table 4.

Table 4. Properties of steel used as reinforcement and shear connectors in the FEA

Diameter	***σ_y (MPa) Initial Yield Stress***	***P_t (MPa) Stress at ultimate***	***ε Strain at failure***	***E_s (kN/mm²)***	***P (kg/m³)***	***v***
6 mm	359	374	0.0049	200	7,700	0.3
9 mm	343	381	0.0061	200	7,800	0.3

3.3 Normal Concrete Model

Material properties of normal concrete capping were obtained from the previous researches [4] & [12]. Compressive strength, tensile strength, Young's modulus, mass density and Poisson ratio of normal concrete Grade 25 were tabulated in Table 5.

Table 5. Properties of normal concrete capping in PLFP Model

P_c, (MPa)	***E_s, (GPa)***	***P , (kg/m³)***	**Poisson ratio, *v***
25	26	2,400	0.3

3.4 Expanded Polystyrene Model

In PLFP, polystyrene functions as an insulation layer and it does not play an important role to sustain the loading, so there is no experimental work carried out for its material properties. Thus, the material properties of expanded polystyrene with reference to Texas Foam Inc. [7] are listed in Table 7. Expanded polystyrene with lowest density 16kg/m3 was chosen to be used. According to Texas Foam Inc. [7], polystyrene is a hyper elastic material and therefore it was assigned in FEA as fully elastic model. The mechanical properties of expanded polystyrene depend largely upon density; where in general, the strength characteristic increases with increment of density. However, such variables as the grade of raw material using geometry of the molded part and processing conditions will affect the package properties and performance.

Table 6. Properties of Expanded Polystyrene (Texas Foam Inc, 2011)

E (kN/mm²)	***Mass Density, (kg/m³)***	***Poisson ratio, v***
0.8963	16	0.4

4. Loading and Analysis Control

The panel bottom was constrained at the reference point of concrete capping in X, Y and Z direction while the top portion was constrained at reference point of concrete capping in X and Z direction. Displacement was assigned at

Y direction at the reference point on the rigid body to simulate the applied loading on the top of the panel. From the applied vertical displacement, the equivalent axial loading applied on PLFP panel can be determined from the history output in the result file. Vertical displacement was increased gradually by using tabular type of amplitude [3] until the panel failed at ultimate load and post failure occurred.

Lastly, the convergence of PLFP model was checked with mesh density study by changing the mesh density to obtain the final mesh size for the FE model. The critical output parameters from the FEA were compared to the experimental results from Mohamad [12]. The field output parameter namely deflection, stress, strains and loading versus time were defined.

5. Results and Discussion

The PLFP model with single shear truss connectors was used from previous experimental results [12] for the calibration purpose. The designation and properties of the model are listed in Table 8. Two panels with slenderness ratio of 28 were chosen to validate the PLFP model.

Table 7. Designation of foamed concrete of PLFP with single shear truss connectors

Panel	*H x W x t*	$\frac{H}{t}$	*Foamed concrete, t_1 (mm)*	*Poly-styrenet$_2$*	Concrete cover, *c*(mm)	*Reinforcement (Vertical and Horizontal)*	*Diameter of Shear Connector*
PLFP1	2,800 x 750 x 100	20	40	20	15	9 mmΦ@150 mm c/c	R6
PLFP2	2,800 x 750 x 125	20	40	20	15	9 mmΦ@150 mm c/c	R6

5.1 Analysis Procedure

In performing the quasi-static analysis, the load was specified by a prescribed maximum vertical displacement at the reference point of rigid body on top of the PLFP panel where the actual axial loading was applied. ABAQUS/Explicit module is a dynamic analysis program and since a quasi-static solution is desired, the prescribed displacement was increased gradually to eliminate any significant inertia effect.

According to Abdullah et al. [13], before any result is accepted, kinetic energy should be compared with internal energy of the whole model throughout the analysis period to give a general indication with the quasi-static solution. The quasi-static response is ensured by keeping the kinetic energy level due to the movement of the model to below 5% of the internal energy at any instance during the time step period as shown in Figure 2.

At the initial development of the model, the analyses were made using coarse mesh to determine a good combination of material properties and to obtain an admissible quasi-static solution. For each trial combination of material properties, the analyses were given by varying the time step period. For each result, the internal and kinetic energies of the whole model were plotted. Figure 3 depicts a typical internal energy levels during the analysis period for the dynamic response while Figure 2 is for the quasi-static response.

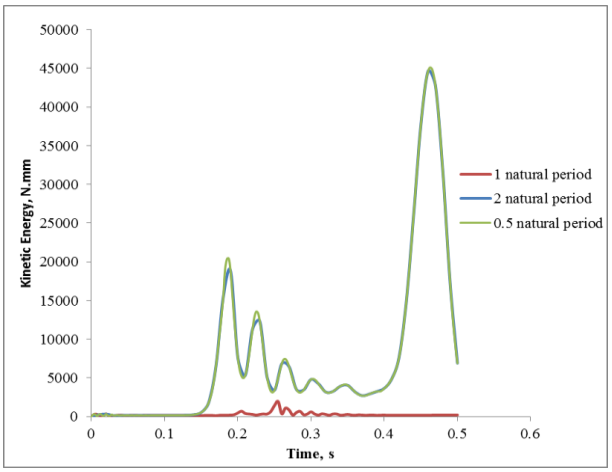

Figure 3. Energy level of the whole model for analysis with 1 natural period.

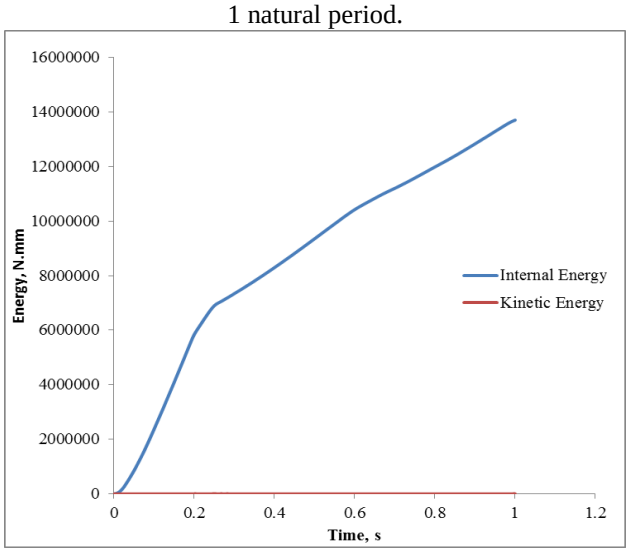

Figure 4. Kinetic energy level of the whole model for analysis with several natural periods

5.2 Convergence Study of PLFP Panel

The quasi-static analysis procedure was further conducted with several element sizes as listed in Tables 9 to illustrate mesh sensitivity. Same material properties were used for all mesh sizes. Results of the analyses using different mesh density were plotted as shown in Figure 4. The graph shows that the models were sensitive to the element size. The response converged to a near constant value when the number of element reached 60,000. Load versus vertical displacement showed similar trend for model with global size 15, 14 and 13 thus the suitable mesh density chosen for parametric study was global size 15 to 14 or about 70,000 to 90,000 elements. The difference in element number was due to size difference of PLFP panel.

Table 8. Result of mesh refinement study of PLFP1

Mesh Size for foamed concrete	*Total Elements*	*F_c (kN)*	*% Difference from Experiment*
Experimental	-	583	-

Data			
GB150	1,124	735	26.07%
GB100	1,725	720	23.50%
GB46	4,894	698	19.73%
GB30	10,248	691	18.52%
GB22	25,483	678	16.30%
GB20	31,305	677	16.12%
GB15	70,305	668	14.58%
GB14	82,507	668	14.58%
GB13	106,264	666	14.24%

Note: GB = global size for mesh density in ABAQUS

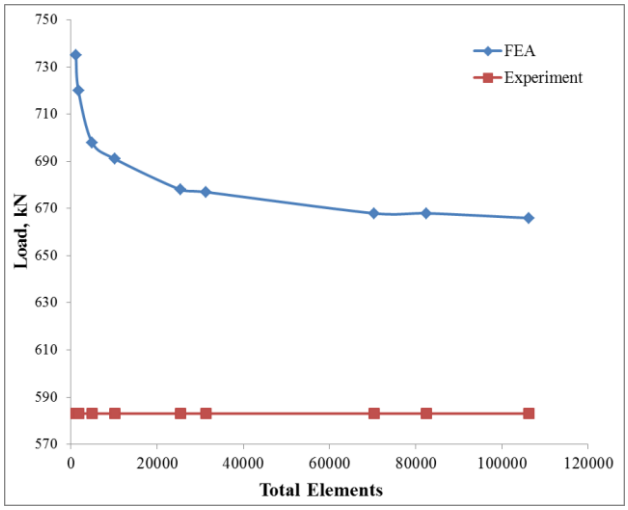

Figure 5. Meshes density study of FEA for PLFP with single shear truss connectors, PLFP1

5.3 Analysis Result for Perfect Model

A perfect FE model (no initial curvature) is compared with the test specimen. The initial analysis result shows that the brittle concrete damage plasticity model is sufficient for modelling foamed concrete used to construct the PLFP. The quasi-static analysis method is capable of predicting the load-deflection behaviour, failure mode and the ultimate load of composite PLFP accurately.

As tabulated in Table 10, results of two PLFP with single shear truss connectors from British Cement Association [11] were used to calibrate the FE model. From the results, the FE model predicted the load carrying capacity within acceptable range which was 3.78% and 14.58% respectively.

Table 9. Ultimate load carrying capacity of PLFP with single shear truss connectors

Panel	$\frac{H}{t}$	*Ultimate Load (kN)*		$\frac{Pu(FEA)-Pu(EXP)}{Pu(EXP)} x\ 100\%$
		Experiment	FEA (perfect model)	
PLFP1	28	583	668	14.58%
PLFP2	22.4	660	685	3.78%

Figure 5 depicts the similarity of the concrete degradation status obtained from FEA and experiment, where crushing of the panel had occurred at the mid height section. In this study, concrete damaged plasticity was chosen as the failure criterion to represent the concrete softening in both tension and compression. Since the loading applied on the panel was axial load thus the panel failed mainly under compression as seen in Figure 5. DAMAGEC is the damage parameter of concrete damaged plasticity that presents the stiffness degradation of foamed concrete respond to compression. Contour of DAMAGEC presents the damage and crack pattern of foamed concrete wythes right after the panel reaches ultimate load carrying capacity.

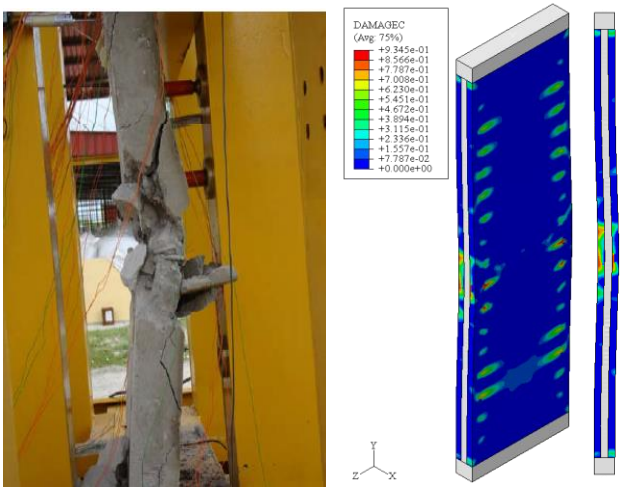

(a) Experiment (b) FEA

Figure 6. Failure Mode of PLFP from Experiment and FEA for PLFP2

5.3.1 Load versus Vertical Displacement Profile

The load versus vertical displacement at load point as shown in Figure 6 depicts the similar trend between FE and experimental results. The load-vertical displacement curve from FEA is able to distinguish the elastic, plastic and damage behaviours of the perfect condition of PLFP model.

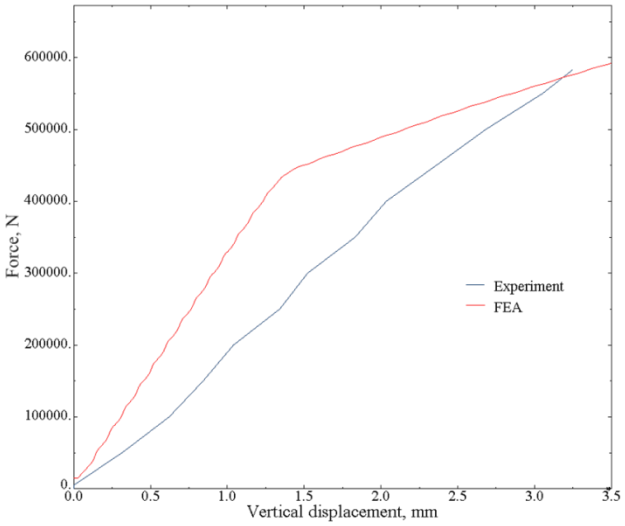

Figure 7. Load versus vertical load displacement for PLFP1.

5.3.2 Load versus Horizontal Displacement Profile

Figure 7 shows the load versus horizontal displacement curve for PLFP1 specimen obtained from experiment and from FEA. It can be seen that the test specimen had deflected as early as the load was applied while the FEA result does not show any movement until reaching the ultimate load. The difference was due to the imperfection of the test specimen. In experiment, the post failure curve could

not be measured due to the brittle mode of failure. On the other hand, the FEA results indicate that the panel behave in the rigid perfectly plastic as of Euler buckling mode where the panel's horizontal displacement showed the panel almost no movement at mid height section in elastic stage and buckled suddenly upon reaching the ultimate load. In FEA, the post failure mode of PLFP panel was measured and the value of horizontal displacement was higher than at' elastic stage after the ultimate load. At elastic stage, the model in FEA is very stiff with almost no horizontal displacement.

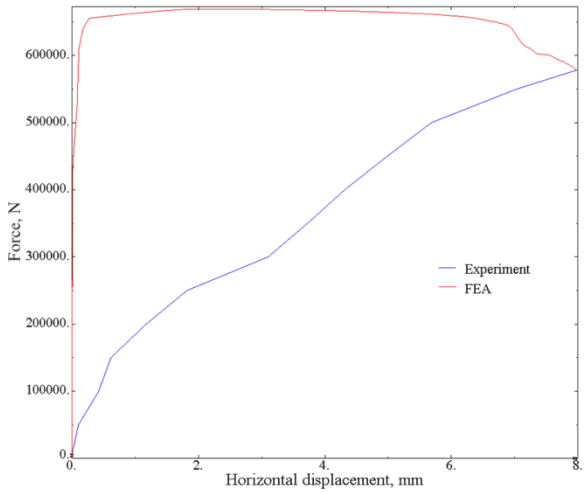

Figure 8. Comparison of FEA and experimental results of load versus horizontal load displacement for PLFP1

5.4 Result Analysis for Imperfect PLFP Mode

In real construction practice, it is nearly impossible to obtain a perfect panel without initial imperfection such as geometrical imperfection, material imperfection or load eccentricity. Therefore, imperfections from experimental works were due to multiple imperfection factors. However, this study focused on the geometrical imperfection with initial eccentricity which is the commence imperfection.

As such, the panel with initial curvature which is the common imperfection condition as stated by American Concrete Institute [14] and British Standard Institution [15], was developed and analysed in order to study the behaviour of a panel in a more realistic condition. Initial curvature variation from $\frac{t}{20}$ to $\frac{t}{6}$ was applied according to American Concrete Institute [14] and British Standard Institution [15]as shown in Figure 8.

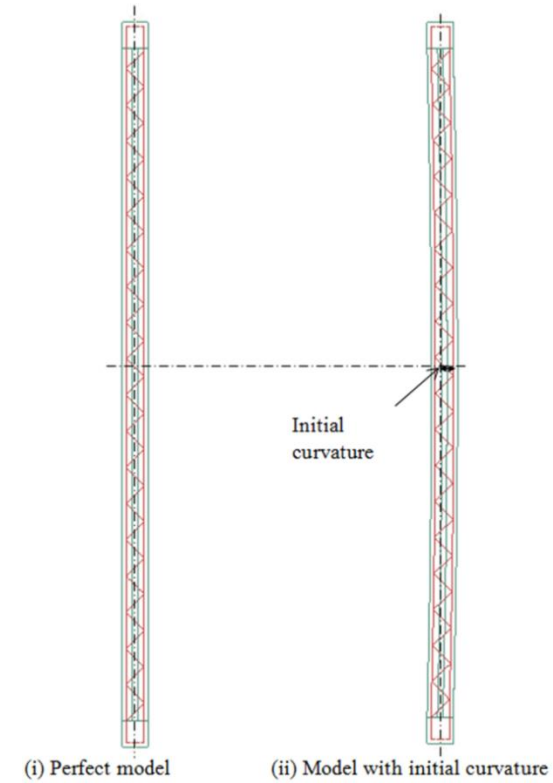

Figure 9. Perfect model and imperfect model of PLFP panel

Table 11 shows the results of FEA of PS1 panel under variable initial curvature. Model with $\frac{t}{12}$ initial curvature at the middle of panel gives the nearest result compared to experimental result, and therefore $\frac{t}{12}$ was chosen as the ideal initial curvature to further study the structural behaviour of PLFP panel. Model with initial curvature was able to predict the higher ultimate strength more accurately compared to perfect model. Comparison of horizontal displacement from experimental and the FEA results is depicted in Figure 9 which also affirms that the behaviours of imperfect model is closer to the experimental result. It is proven that imperfect model from FEA is able to represent the experimental PLFP result more accurately.

Table 10. Imperfection study of PLFP by FEA

Imperfection	*F_c (kN)*	*Difference of F_c (kN)*	*% Difference from Experiment*
Experimental Data	583	0	-
0 imperfection	668	85	14.58%
t/6	531	52	8.92%
t/8	557	26	4.56%
t/10	575	8	1.37%
t/12	586	3	0.51%
t/15	599	16	2.74%
t/20	614	31	5.31%

Note : Imperfection was determined by the initial eccentricity of PLFP1

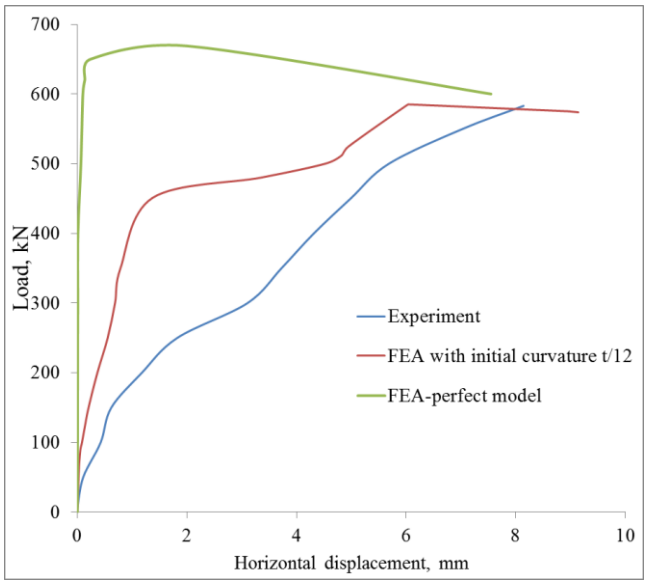

Figure 10. Load versus horizontal displacement at mid height section from experiment and FEA of PLFP1

5.5 Post Failure Mode

After the panel reached its ultimate load carrying capacity, it entered the post failure stage. Figures 10 and 11 show the failure and the post failure stages of panels when axial loading was applied. Loading was applied to the panel until 50 mm vertical displacement occurred in order to investigate the damage pattern and stress distribution of a panel from pre-damaged stage to post failure stage. Failure stages were illustrated in six phases from the vertical displacement increment applied in FEA which were 0 mm, 5 mm, 15 mm, 30 mm, 40 mm and 50 mm to visualize and predict the panel condition from pre-damaged condition to damaged condition in post failure stage due to axial loading.

During the pre-damaged stage, damage and crack pattern of a panel is located at the highest stress distribution zone after reaching the ultimate load. In order to study their relationship, the contour of damage criteria and stress distribution from pre-damaged to post failure stages are shown in Figures 10 and 11. It can be seen that, after the panel was damaged, the damage zone expanded with the increment of vertical displacement applied at the top support. Red colour zone in the damage status contour represents the crushing and damage zone. On the other hand, as seen in Figure 11, stress distribution in the panel switched to other pre-damaged zone after the panel entered post failure stage because the damaged zone of the panel was not capable to sustain the applied load after being damaged.

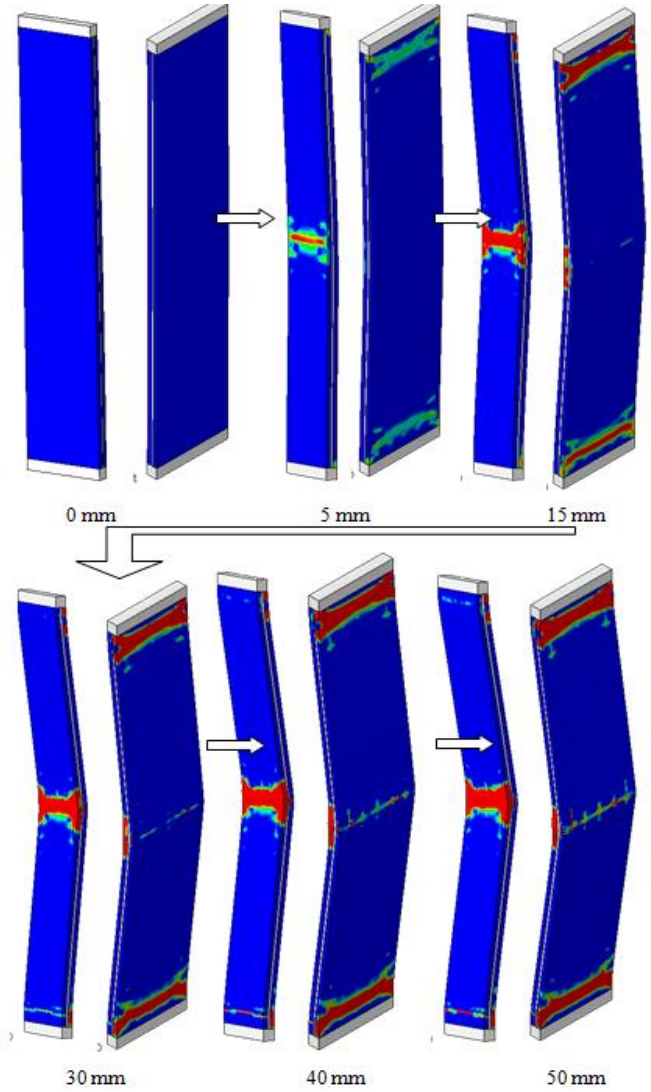

Figure 11. Damage status of PLFP-11 vertical displacement increments from 0 mm to 50 mm

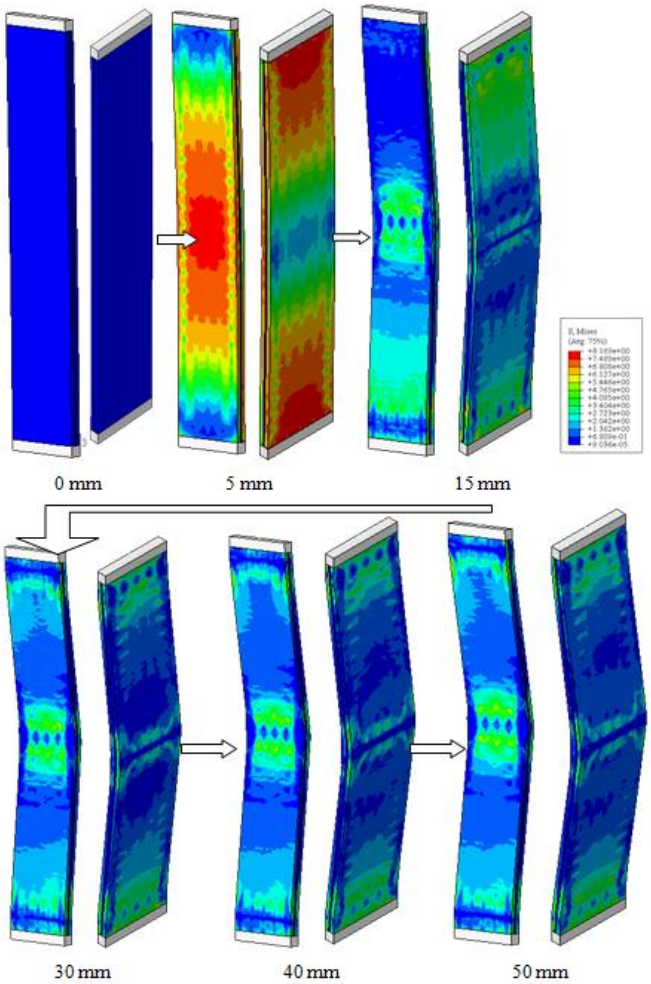

Figure 12. Stress distribution of PLFP-11 vertical displacement increments from 0 mm to 50 mm

Other than that, the horizontal displacement of a panel from pre-damaged stage to damaged stage is visualized in Figure 14. It can be seen that, the horizontal displacement and the bending at the mid height section increased proportionally with the increment of vertical displacement applied on top of a panel.

6. Conclusion

Quasi static response of precast lightweight foamed concrete sandwich panel subjected to axial compression is studied using ABAQUS/Explicit module. The proposed model concrete damaged plasticity which is only available in this software package, and it is sufficient for modelling concrete behaviour under compression. Perfect model of PLFP is able to predict the structural behaviour of PLFP under perfect condition. However, the initial geometrical imperfection due to construction always happens in reality. Therefore, it is very important to taken into account the geometrical imperfection in order to study the actual behaviour of PLFP.

The method for modelling the PLFP subjected to axial compression is proposed in this study. Due to the brittle natural of the foamed concrete used to construct the PLFP panel, quasi static analysis using concrete damaged plasticity material model was found to be suitable for modelling the PLFP panel. In order to obtain good results that can represent the real structure, the imperfect model with $\frac{t}{12}$ initial horizontal deflection at the mid height should be used.

Therefore, a computational study by using FEA can be used as an economic alternative investigation tool to replace experimental work to study structural behaviour of wall system

Acknowledgements

The author would like to thank University Tun Hussein Onn Malaysia for its financial support. Centre for Information and Communication Technology (CICT) of Universiti Teknologi Malaysia for supporting and providing facilities and services of high performance computing.

References

[1] J. D. Artizabal-ochoa, "Stability and Second order non-linear analysis of 2D multi-column systems semi rigid connections: Effects of Initial Imperfections,'' *International Journal of Non-linear Mechanics.* vol. 47, no. 5, pp. 537-560, 2012.

[2] N. Boissonnade, H. Somja, "Influence of Imperfections in FEM Modelling of Lateral Torsional Buckling,'' *Proceeding of the Annual Stability Conference Structural Stability Research Council.* Gravevine, Texas, pp. 1-15, Apr. 2012.

[3] *Abaqus 6.9 Documentation*, Dassault Systemes, Abaqus, Inc., United States, 2009.

[4] S. N. Mokhatar, R. Abdullah, "Computational Analysis of Reinforced Concrete Slabs Subjected to Impact Loads,'' *Int J. Of Integrated Engineering*, vol . 4, no. 2, pp. 70-76, 2012.

[5] C. M. Newberry, J. M. Hoemann, B. T. Bewick, J. S. Davidson, "Simulation of Prestressed Concrete Sandwich Panels Subjected to Blast Loads,'' *2010 Structures Congress*, Orlamdo, Florida, May 12-15, 2010.

[6] W. I. Goh, N. Mohamad, R. Abdullah, A. A. A. Samad "Compression Test and Finite Element Analysis of Foamed Concrete Cube,'' *The Journal of Engineering and Technology (JET)* vol. 5, no. 1, pp. 1-10, 2014.

[7] Expanded Polystyrene (E.P.S) Handbook. Texas Foam Inc., 2011.

[8] T. Jankowial, T. Lodygowski, "Quasi static failure criteria for concrete,'' *Foundations of Civil and Environmental Engineering*, vol. 6, pp. 53-69. ISSN 1642-9303, 2005.

[9] L. Jason, G. P. Cabot, A. Huerta, S. Ghavamian, "Damage and Plasticity for concrete behavior,'' *European Congress on Computational Methods in Applied Sciences and Engineering*, German. *ECCOMAS 2004*, pp1-16, 2004.

[10] J. Lee, G. Fenves, "Plastic-Damage Model for Cyclic Loading of Concrete Structures," *J. Eng. Mech.*, vol. 124, no. 8, pp. 892–900, 1998.

[11] British Cement Association, *Foamed Concrete Composition and Properties.* pp. 165-168. British Cement Association, 1994.

[12] N. Mohamad, "The Structural Behavior of Precast Lightweight Foamed Concrete Sandwich Panels as Load Bearing Wall,'' Ph.D Thesis, Universiti Teknologi Malaysia, 2010.

[13] R. Abdullah, P. Vidal, Paton-Cole, W. Samuel Easterling, F. ASCE, "Quasi-static Analysis of Composite Slab,'' *Malaysian Journal of Civil Engineering*, vol. 19, no. 2, pp. 94-102, 2007.

[14] American Concrete Institute. *Building Code Requirements for Reinforced Concrete and Commentary-ACI 318-89* (Revised 1992), Michigan, ACI 318-89, 1992.

[15] British Standard Institution, *Structural Use of Concrete BS8110.* London: BS 8110-1, 1997.